Brain Research 1748 (2020) 147122

Contents lists available at ScienceDirect

Brain Research

journal homepage: www.elsevier.com/locate/brainres

Research report

Longitudinal multiparametric MRI study of hydrogen-enriched water with minocycline combination therapy in experimental ischemic stroke in rats

Zhao Jiang[a], Tharun T. Alamuri[a], Eric R. Muir[a], Dennis W. Choi[b], Tim Q. Duong[a,*]

[a] Departments of Radiology, Stony Brook Medicine, Stony Brook, NY 11794, United States
[b] Departments of Neurology, Stony Brook Medicine, Stony Brook, NY 11794, United States

HIGHLIGHT

- H_2 therapy reduced infarct volume in both H_2 and H2M groups compared to controls at 1 and 7 days after stroke.
- Both H_2 and H2M improved neurologic functional recovery on day 7 after stroke.
- H2M treatment attenuated post-stroke hyperperfusion in hyperacute phase.
- H_2 minimized and H2M markedly minimized white matter injury after stroke.

ARTICLE INFO

Keywords:
Stroke
Hydrogen
Antioxidant
Cerebral blow flow
Diffusion tensor imaging
Neuroprotection

ABSTRACT

Free radicals are downstream mediators of several cytotoxic cascades contributing to ischemic brain injury. Molecular hydrogen (H_2) is an antioxidant potentially useful in the treatment of stroke. Hydrogen is easy to deliver, biologically non-toxic and diffuses freely through all biological structures including the blood-brain barrier and cellular membranes. This study evaluated the efficacy of hydrogen treatments in a rat stroke model compared to vehicle-treated controls using multiparametric MRI and neurological tests. Additionally, comparison of H_2 treatment alone was made with H_2 combined with minocycline (H2M) treatment (12 rats per group). The primary findings were: i) H_2 therapy reduced infarct volume in both H_2 and H2M groups compared to controls at 1 and 7 days after stroke, and ii) both H_2 and H2M improved neurologic functional recovery on day 7. The secondary outcomes were: iii) H2M treatment attenuated post-stroke hyperperfusion in the hyperacute phase, and iv) H2M markedly minimized white matter injury. In conclusion, this is the first study to use MRI to longitudinally study H_2 and H2M treatment on ischemic stroke and the first study to compare H_2 treatment combined with another potential stroke therapeutic (H2M).

1. Introduction

Free radicals are downstream mediators of several cytotoxic cascades contributing to ischemic brain injury (Chan, 2001), including excitotoxicity (Coyle and Puttfarcken, 1993; Monyer et al., 1990) and inflammation (Iadecola and Alexander, 2001). Furthermore, the significance of free radicals to stroke pathogenesis is likely to increase with current stroke treatments to re-establish cerebral blood flow (such as recombinant tissue plasminogen activator and endovascular clot retrieval therapy) being increasingly deployed in stroke centers, since reperfusion after stroke enhances the formation of free radical species (Kuroda and Siesjo, 1997).

The search for an antioxidant treatment for stroke is still ongoing. Several candidate drugs, including tirilazad mesylate, NXY-059, and Ebselen® were advanced to clinical trials in stroke patients, but were abandoned after disappointing results (Ginsberg, 2009). The antioxidant Edavarone® gained approval for the treatment of acute stroke in Japan, but evidence supporting its effectiveness is limited (Feng et al., 2011). Past disappointments do not disprove the rationale for antioxidant use in stroke, as the antioxidants tested to date have significant limitations in terms of radical scavenging profile or ability to access all relevant cellular compartments; specific trial design issues have also been raised (Ginsberg, 2009).

More recently, molecular hydrogen was identified as another antioxidant potentially useful in the treatment of stroke (Ohsawa et al., 2007). Its chemical redox properties were previously known, but it did not attract the interest of biologists until Ohta and colleagues demonstrated that the administration of 2% H_2 gas by inhalation reduced

* Corresponding author at: Stony Brook Medicine, Radiology, HSC Level 4, Room 120, 101 Nicolls Rd, Stony Brook, NY 11794-8460, United States.
E-mail address: Tim.Duong@einsteinmed.org (T.Q. Duong).

https://doi.org/10.1016/j.brainres.2020.147122
Received 21 May 2020; Received in revised form 6 September 2020; Accepted 7 September 2020
Available online 11 September 2020
0006-8993/

brain infarction and behavioral deficits in a rat stroke model (Ohta, 2014). These investigators noted that hydrogen has highly favorable properties for use as a medical antioxidant. It scavenged the highly reactive mediators of pathological oxidative stress, peroxynitrite and hydroxyl radicals, while showing little reactivity with radical species or oxidized metabolites important to normal cellular signaling, including superoxide, hydrogen peroxide, nitric oxide, and oxidized nicotinamide adenine dinucleotide (NAD+) (Ohsawa et al., 2007). Protective effects of hydrogen were also observed in different experimental brain injury models (Cui et al., 2014; Hugyecz et al., 2011; Li et al., 2012, 2019; Liu et al., 2011; Nemeth et al., 2016). Furthermore, hydrogen has cytoprotective effects against insults other than ischemia and in organs other than the brain (Ohta, 2014; Zhang et al., 2018). More recent studies have also shown H_2 treatment has further neuroprotective effects, such as reducing inflammation and suppressing apoptosis (Li et al., 2019; Zhang et al., 2019). Hydrogen is easy to deliver via inhalation of a gas mixture or dissolved in water or saline. Hydrogen is biologically non-toxic and diffuses freely through all biological structures including the blood-brain barrier and cellular membranes, reaching all biological compartments (Ohta, 2014). In addition to animal studies, in a small randomized controlled trial, 25 patients with mild acute stroke (NIH Stroke Scale score 2–6) who were treated with 3% H_2 inhalation were reported to have a better outcome (lower NIH Stroke Scale at days 3–14 compared to controls) (Ono et al., 2017). There are also a few on-going clinical trials (i.e., NCT03320018).

One of the reasons clinical stroke neuroprotection has been so difficult to achieve may be the multiplicity of ischemic injury pathways. Virtually all clinical drug trials (and most experimental studies) to date have deployed single agents. While the evidence supporting the potential value of hydrogen as a treatment for stroke is growing, many other candidate therapies have ultimately failed to prove efficacious in clinical trials. We decided therefore to evaluate if the addition of the semisynthetic tetracycline antibiotic, minocycline, could enhance hydrogen-induced ischemic neuroprotection in an experimental stroke model.

Minocycline is readily available, safe, and beneficial in animal stroke models (Yrjanheikki et al., 1999), and may be borderline effective in human stroke (Malhotra et al., 2018). Its neuroprotective and vasculoprotective effects are based on a mixture of anti-inflammatory and anti-apoptotic actions (Fagan et al., 2011). At standard antimicrobial doses, minocycline inhibits matrix metalloproteinase-9 (MMP-9), which is overexpressed and released from multiple cell types post ischemia, contributing to inflammation, blood-brain barrier breakdown, and cell death (Chaturvedi and Kaczmarek, 2014). Additionally, minocycline potently inhibits poly(ADP-ribose) polymerase-1 (PARP), which is overactivated by oxidative DNA damage and can promote cellular energy depletion and "parthanatos" (Dawson and Dawson, 2018). PARP is a downstream mediator of acute zinc toxicity (Sheline et al., 2003), another pathway implicated in ischemic cell death (Koh et al., 1996). Lastly, minocycline has been found to reduce infarct size and NLRP3 inflammasome activation (Lu et al., 2016; Xu et al., 2004), and improve neurological functioning and recovery (Hewlett and Corbett, 2006).

MRI has become a standard method to evaluate the extent of injury in the brain after stroke. T_2 MRI provides final infarct volume in the subacute and chronic phases in vivo (Shen et al., 2013). Perfusion and diffusion MRI provides for early diagnosis of ischemic stroke, as well as for the longitudinal evaluation of therapeutic efficacy in chronic stroke (Sorensen et al., 1996, 1999). Ischemic stroke occurs when basal cerebral blood flow (CBF) drops below a critical threshold (~0.2 ml/g/min) (Astrup et al., 1981a, 1981b; Hossmann, 1994; Lo et al., 2005), resulting in metabolic energy failure and cellular swelling. These changes rapidly precipitate a reduction of the apparent diffusion coefficient (ADC) of water in the brain (Minematsu et al., 1993; Moseley et al., 1992, 1990). During early ischemic injury, a central core of severely compromised CBF and severe ADC reduction is typically surrounded by tissue with moderately diminished CBF, near normal ADC, and impaired electrical activity but preserved cellular metabolism (Shen et al., 2013). The difference in anatomical area defined by perfusion- and diffusion-weighted MRI is commonly referred to as the "perfusion-diffusion" mismatch (Kidwell et al., 2003; Warach, 2003), which approximates the "ischemic penumbra" (Astrup et al., 1981a, 1981b; Hossmann, 1994; Lo et al., 2005). Early interventions in stroke patients and experimental stroke models have been shown to salvage some mismatch tissue in a time-dependent manner in animal models of stroke (Shen et al., 2013) and in humans (Kidwell et al., 2003, 2000; Warach, 2003). The mismatch concept has been used to select patients for treatment who will likely benefit from thrombolytic therapy and/or mechanical clot retrieval (Albers, 1999; Davis and Donnan, 2009; Kidwell et al., 2001). Recent evidence indicates that proper patient selection for acute stroke treatment is critically important to achieve positive outcomes. Thus, MRI plays a critical role in targeting treatment to specific stroke patients.

Given the potential neuroprotective effects of H_2, the overall aim of this study was to investigate the longitudinal efficacy of H_2 and H2M-combination treatments in the rat middle cerebral artery occlusion (MCAO) stroke model, using non-invasive and clinically relevant MRI techniques. The goals of this study are: i) to evaluate the efficacy of hydrogen treatment in a rat stroke model, and ii) to evaluate if minocycline added to hydrogen treatment (H2M) could further improve efficacy. The readouts were multiparametric MRI and neurological scoring. Comparisons were made with vehicle-treated controls.

2. Results

2.1. Effects of H_2 on lesion volume

Representative MRI of the apparent diffusion coefficient (ADC), cerebral blood flow (CBF), and T_2 maps at multiple time points after MCAO from the control, H_2, and H2M groups are shown in Fig. 2. ADC and CBF were reduced in the area of ischemic injury. ADC maps at 30 mins after MCAO (prior to treatment) were similar across all 3 groups, showing a reproducible MCAO model. T2 lesion were hyperintense (higher T2) at 1 and 7 days after stroke. T2 was higher at 1 day after stroke as vasogenic edema was more severe compared to that at 7 days after stroke. T2 lesion volumes were smaller in the H2 and H2M group compared to those in the vehicle group.

The quantitative core lesion volume group data at multiple time points at 30 and 90 mins and at 1 and 7 days after stroke onset are summarized in Fig. 3. At 30 mins, the initial ADC-defined lesion volumes before treatment were not statistically different from each other (223.7 ± 23.8 mm^3 for control, 212.6 ± 23.6 mm^3 for H_2, 200.9 ± 20.4 mm^3 for H2M, $p > 0.05$). At 90 mins after MCAO (30

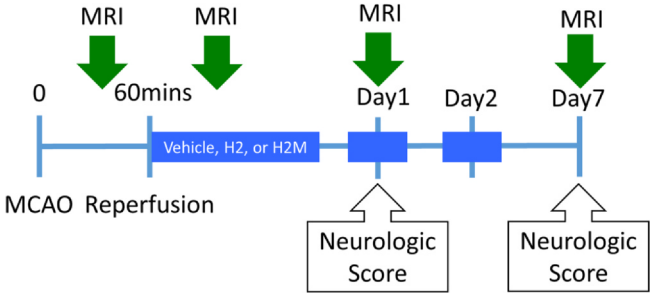

Fig. 1. Experimental Design. MCAO was induced at time 0 and reperfusion occurred at 60 mins after MCAO. There were three treatment (vehicle, H_2, or H2M) groups. Treatments were given directly after reperfusion, and again on days 1 and 2 after stroke. MRI was obtained at ~30 mins after MCAO (before treatment), again at 90 mins (after first treatment), and at 1 and 7 days after MCAO on the same animals (green arrows). Neurological scores were obtained on 1 and 7 days after MCAO.

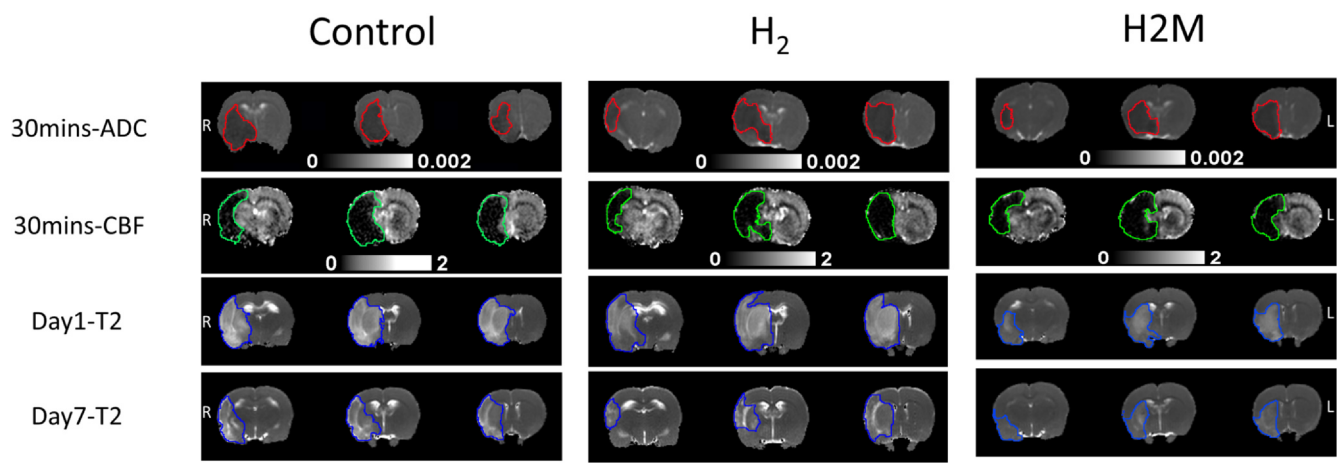

Fig. 2. Representative ADC, CBF and T2 maps from individual animals from the control, H_2, and H2M groups. ADC and CBF maps are from 30 mins after MCAO, and T_2 maps are from 1 and 7 days after MCAO. Red contours outline the region of abnormal ADC pixels. Green contours outline the region of abnormal CBF. Blue contours outline the region of abnormal T2. R: right, L: left. Scale bar shows ADC: 0 to 0.002, and CBF 0 to 2.

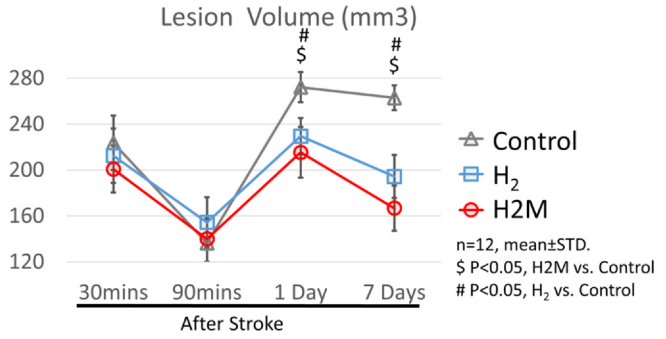

Fig. 3. Longitudinal lesion volumes of different treatment groups. Lesions volumes at 30 and 90 mins after MCAO were measured by ADC. Lesions volumes at 1 and 7 days after stroke by T2. Data are expressed as mean ± STD, n = 12 each. From two-way repeated measures ANOVA, time and group*time had significant effects on lesion volume ($p < 0.05$). Significant differences from t-tests with Bonferroni-Holm correction are indicated as $ $p < 0.05$ H2M vs control. # $p < 0.05$ H_2 vs control.

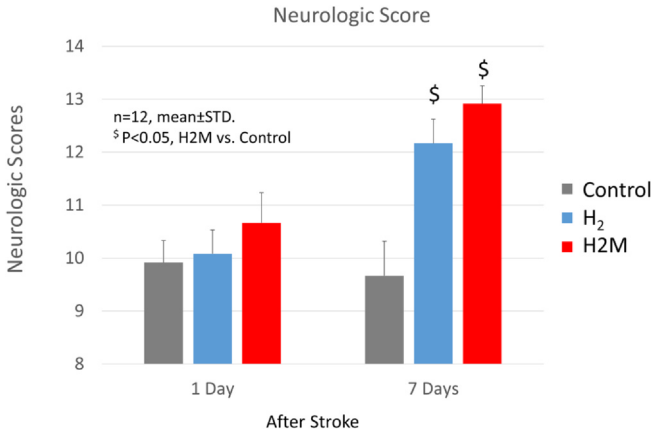

Fig. 4. Neurological scores of the control, H_2 and H2M group (n = 12, mean ± STD). Significant differences from t-tests with Bonferroni-Holm correction are indicated as $ $p < 0.05$ from control.

mins after reperfusion), lesion volumes decreased in all 3 groups.

One day after MCAO, the lesion volumes of all three groups increased. However, lesion volumes of the H_2 and H2M groups were significantly smaller than that of the control group (H_2 = 229.5 ± 15.8 mm^3, H2M = 215.4 ± 22.2 mm^3, control = 272.3 ± 13.0 mm^3; $p < 0.05$ H_2 and H2M compared to control). Seven days after MCAO, lesion volumes of both the H_2 and H2M remained significantly smaller than that of the control (H_2 = 194.4 ± 18.6, H2M = 166.8 ± 19.6 mm^3, control = 263.0 ± 10.7 mm^3, $p < 0.05$ H_2 and H2M compared to control). While the lesion volume of the H2M group trended slightly smaller, there were no significant differences in lesion volumes between H_2 and H2M groups 1 or 7 days after MCAO.

2.2. Behavioral outcomes

Garcia neurological scores were analyzed in a blinded fashion at 1 and 7 days after stroke onset (Fig. 4). From two-way repeated measures ANOVA, time ($p < 0.001$), group ($p = 0.007$), and time*group ($p < 0.05$) had significant effects on behavioral changes. The control group demonstrated worse neurobehavioral scores (9.7 ± 0.7) at seven days after MCAO compared to both treatment groups (H_2 = 12.1 ± 0.5, H2M = 12.9 ± 0.3, $p < 0.05$).

2.3. Effects of H_2 on cerebral blood flow

CBF from the ischemic core (Fig. 5A) and the perfusion-diffusion mismatch region (Fig. 5B) were measured at 30 mins, 90 mins, and 1 and 7 days after stroke. At 30 mins post MCAO (prior to reperfusion), the normalized CBF values of both core and mismatch were low and not statistically different among the 3 groups. At 90 mins after MCAO (30 mins after reperfusion), normalized CBF values from mismatch and core recovered and were similar among the three groups.

From two-way repeated measures ANOVA, time had significant effects on CBF in the mismatch region ($p < 0.001$) but not time*group ($p = 0.08$). There was still significant difference between groups ($p = 0.005$). There were no significant differences between groups in the core region. At one day after MCAO, in the mismatch region, CBF of the treatment groups (H_2 = 0.885 ± 0.057 and H2M = 0.891 ± 0.058 ml/g/min) was significantly lower than that of the control group (1.162 ± 0.098 ml/g/min, $p < 0.05$). Treatment prevented hyperperfusion after reperfusion. At 7 days after MCAO, in the mismatch region, normalized CBF of the H_2 group (0.892 ± 0.031 ml/g/min) was significantly lower ($p < 0.05$) than the H2M group (1.113 ± 0.086 ml/g/min) and the control group (1.084 ± 0.067 ml/g/min). The H_2 group still showed mild hypoperfusion, suggesting that the minocycline in the H2M group helped to normalize CBF between 1 and 7 days post-stroke.

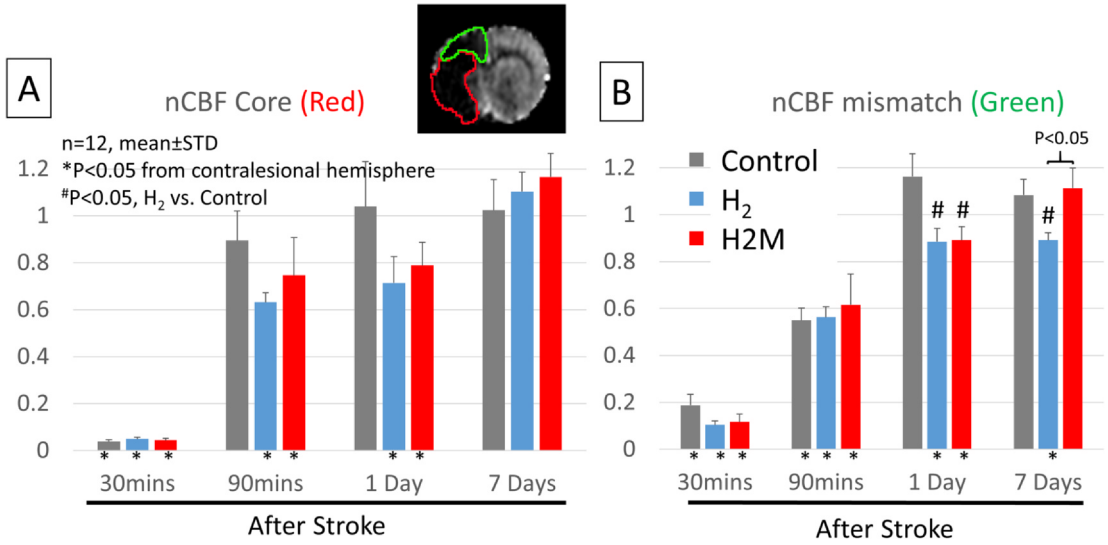

Fig. 5. Normalized CBF in the ischemic core and the perfusion-diffusion mismatch at 30 mins, 90 mins, 1 and 7 days after MCAO. CBF was normalized against values obtained in the contralesional hemisphere. Data are expressed as mean ± STD, n = 12 per group. Significant differences from t-tests with Bonferroni-Holm correction are indicated as # $p < 0.05$ versus control. * $p < 0.05$ from contralateral CBF from uncorrected paired t-tests. Note that the ROIs of the ischemic core and perfusion-diffusion mismatch were defined at 30 mins after MCAO, and the same ROI was applied to all time points.

2.4. Effects of H_2 on white matter integrity

White matter integrity of the corpus callosum was assessed from diffusion MRI from which fractional anisotropy (FA), mean diffusivity (MD), radial diffusivity (RD), and axial diffusivity (AD) were calculated (Fig. 6). The FA values in both hemispheres were significantly affected by time ($p < 0.001$) but not treatment group or time*group factors ($p > 0.05$) using two-way repeated measures ANOVA (Fig. 7A).

The MD values from two-way repeated measures ANOVA were significantly affected by time ($p < 0.001$) but not time*group ($p > 0.05$) in both hemispheres. However, there was significant difference between groups ($p = 0.046$) in the ipsilesional hemisphere but not the contralesional side. MD values of the H2M group were significantly lower compared to those of the H_2 group ($p < 0.05$) in the corpus callosum of both hemispheres (Fig. 7B) on the first day, and in the ipsilesional hemisphere on the seventh day. H2M was also significantly lower than control in the ipsilesional hemisphere on the seventh day ($p < 0.05$).

RD values from two-way repeated measures ANOVA result were significantly affect by time ($p < 0.001$) but not time*group ($p > 0.05$) in bilateral hemispheres. However, there was significant difference between groups ($p = 0.008$) in the ipsilesional hemisphere but not the contralesional side. RD values of the H2M group were significantly lower compared to those of the H_2 group ($p < 0.05$) in the corpus callosum of both hemispheres (Fig. 7C) on the first day, and in the ipsilesional hemisphere on the seventh day. H2M was also significantly lower than control in the ipsilesional hemisphere on the first and seventh day ($p < 0.05$).

AD was significantly affected by time ($p < 0.001$) but not time*-group ($p > 0.05$) in bilateral hemispheres from two-way repeated measures ANOVA. However, there was significant difference between groups ($p = 0.046$) in the contralesional but not ipsilesional hemisphere. AD values of the H2M group were significantly lower compared to those of the H_2 group ($p < 0.05$) in contralesional hemispheres (Fig. 7D) on the first day. Collectively, in comparison to the H_2 group, the H2M combination therapy group showed generally improved DTI

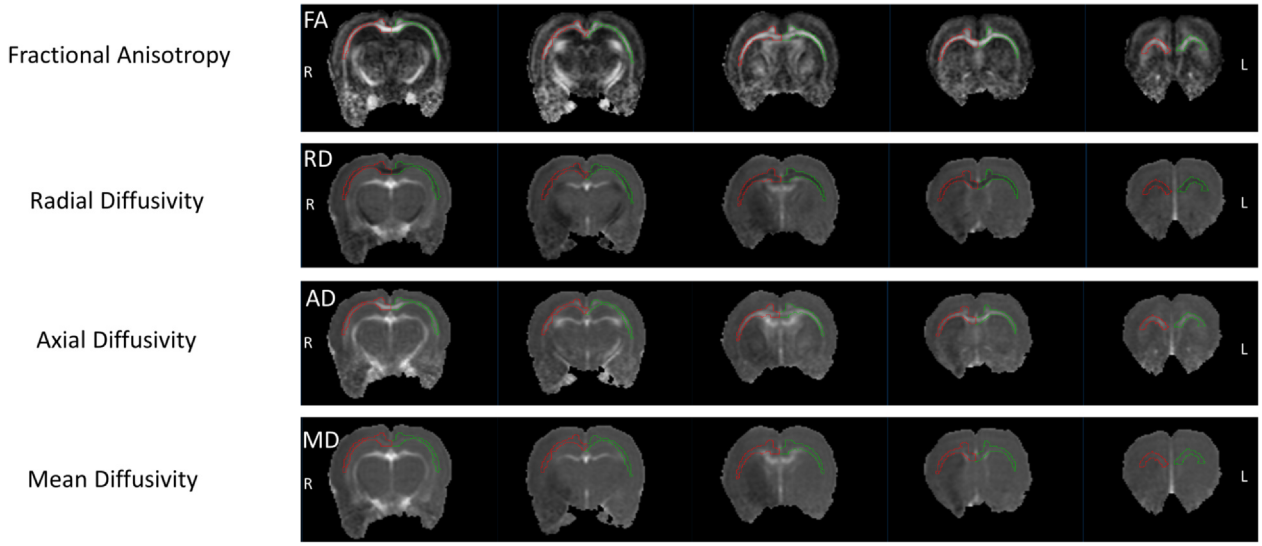

Fig. 6. Representative diffusion data showing FA, MD, RD and AD maps at 30 mins after stroke from one animal from control group. White-matter regions of interest of the corpus callosum from which data were analyzed from the contralesional (green) and ipsilesional (red) hemispheres are shown. R: right, L: left.

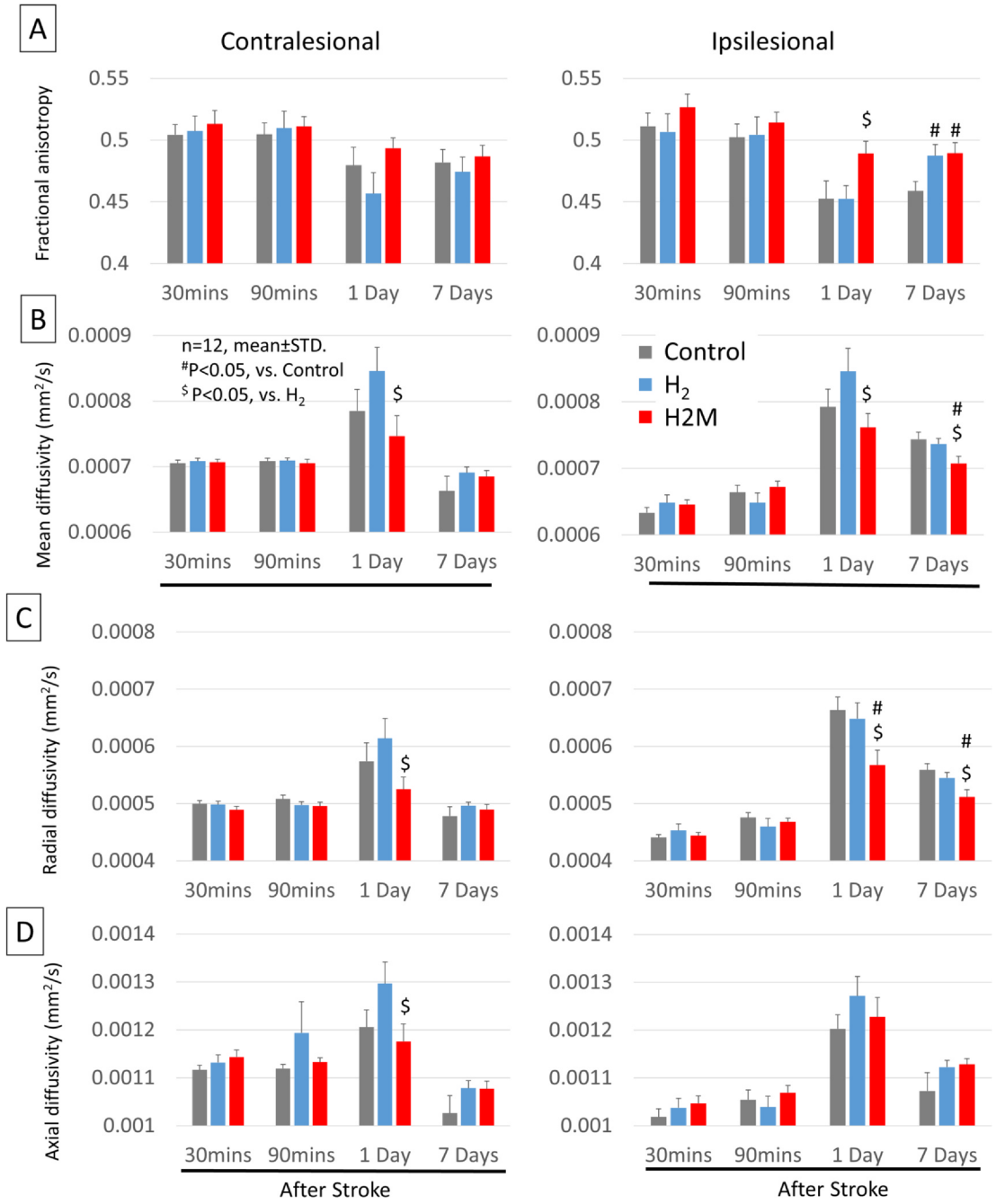

Fig. 7. (A) Fractional anisotropy, FA, (B) radial diffusivity, RD, (C) mean diffusivity, MD, and (D) axial diffusivity, AD in the contralesional and ipsilesional corpus callosum at 30 mins, 90 mins, and 1 and 7 days after MCAO. Data are expressed as mean ± STD, n = 12 in each group. Significant differences from t-tests with Bonferroni-Holm correction are indicated as $p < 0.05 versus H_2. #p < 0.05 versus control.

parameters.

3. Discussion

This double-blinded study applied longitudinal multiparametric MRI and behavioral measurements to assess the progressive treatment effects of H_2 water during the hyperacute to subacute phases of experimental ischemic stroke, and to additionally test the hypothesis that H_2 combination therapy with minocycline could further improve outcomes compared to H_2 treatment alone. The primary findings were: i) H_2 therapy reduced infarct volume in both H_2 and H2M groups compared to controls at 1 and 7 days after stroke, and ii) both H_2 and H2M improved neurologic functional recovery on day 7. The secondary outcomes were: iii) H2M treatment attenuated post-stroke hyperperfusion in hyperacute phase, and iv) H2M minimized white matter injury. To our knowledge, this is the first study to use MRI to longitudinally study H_2 treatment of experimental ischemic stroke, and the first study to examine the neuroprotective benefit of H_2 combined with another potential stroke therapeutic (H2M).

Our major findings are consistent with previous H_2 preclinical studies (H. Li et al., 2019; Ohsawa et al., 2007). Ohsawa et al. compared three different durations of H_2 gas inhalation in a 90 min temporary MCAO rat model, with 85 and 120 min treatments beginning at onset of stroke, and a 35 min treatment starting 5 mins before reperfusion. Interestingly, the latter duration only decreased infarct volume in the striatum, while the former two durations decreased infarct volume in

both striatum and cortex, suggesting treatment prior to reperfusion, while not always possible clinically, may provide additional benefit. These previous findings together with ours indicate that H_2 treatment could be protective against ischemic stroke. Additionally, minocycline has also been shown to be neuroprotective even when given before ischemia (Jin et al., 2015; Naderi et al., 2017; Tanaka et al., 2018). Hydrogen and minocycline individually have excellent safety profiles in humans, so both H_2 or H2M could potentially be administered by emergency responders.

3.1. H_2 and H2M treatment effects on lesion volume and behavioral outcomes

H_2 treatment reduced MRI-defined lesion volumes and improved both 1 and 7 day neurological scores compared to control treatment, consistent with previous results (Li et al., 2019; Zhang et al., 2019). Previous results have also found minocycline treatment alone to do the same (Naderi et al., 2020; Sheng et al., 2018). The improvement in neurological scores are consistent and likely the results of reduced lesion volume and reduced white-matter damage. Here we demonstrated that the novel combination of H_2 and minocycline (H2M) was also effective in reducing MRI-defined lesion volume and improving neurological scores. Furthermore, compared to H_2 treatment alone, combination H2M treatment resulted in significantly more normalized 7 day CBF and DTI parameters, as well as a non-significant trend towards further reduction in 7 day lesion volume and improvement in 7 day neurological scores.

In our study, we analyzed the mismatch and the initially abnormal ADC tissue together which were considered broadly as “at risk” tissue, but did not analyzed separately whether the mismatch was salvaged. Our results showed that some initially abnormal ADC tissue was reversible but only transiently in this stroke model (Figs. 2 and 3), consistent with our previous publications (Huang et al., 2018; Jiang et al., 2015). In addition, we further identified the mismatch volume at the initial time point, and determine whether its ADC and CBF (of the same volume) changed at a later time point. This analysis tracked the physiological and biophysical changes of various tissue types longitudinally, not commonly done in clinical stroke studies.

3.2. H_2 and H2M treatment effects on CBF

CBF in the ischemic core during MCAO was markedly reduced relative to normal values and returned towards normal after reperfusion as expected. However, CBF in the ischemic core was not significantly different amongst groups across all time points. This is perhaps not surprising because the tissue in the MRI-defined ischemic core was likely not reperfused after mechanical re-cannulation and likely non-salvageable in this model. Note that ischemic core ROI was defined at 30 mins after MCAO and the same ROI applied to all subsequent time points.

CBF in the perfusion-diffusion mismatch during MCAO was markedly reduced relative to normal values and returned toward normal (but did not reach normal) value after reperfusion. Neither H_2 nor H2M treatment altered tissue perfusion in a consistent manner across all time points, suggests that these treatments might not have direct vasoactive effects in the brain. However, the H_2 and H2M groups did not show hyperperfusion, whereas the control group showed peak hyperperfusion 1 day after MCAO, especially in the mismatch region. Visual inspection of CBF maps often showed clusters of significant hyperperfusion that might not be evident on ROI-averaged and group values. This finding is consistent with previous studies which showed that hyperperfusion peaked around 1–2 days post transient ischemia (Shen et al., 2011; Tanaka et al., 2007). Early immediate post-ischemic hyperperfusion sometimes observed immediately after recanalization is a hallmark of efficient recanalization after stroke (Sundt et al., 1969; Tasdemiroglu et al., 1992). It has been suggested to be both beneficial (i.e., to salvage tissue in and around the ischemic zone or prevent infarct growth) (Marchal et al., 1996) and harmful (i.e., to aggravate edema, hemorrhage and neuronal damage after reperfusion) (Pan et al., 2007; Schaller and Graf, 2004). In contrast, late post-ischemic hyperperfusion is often associated with tissue necrosis (Ackerman et al., 1981; Baron et al., 1981, 1983; Tran Dinh et al., 1997). The spatio-temporal progression of hyperperfusion was highly correlated with T_1, T_2 and blood-brain-barrier changes, although in some animals hyperperfusion preceded T_2 increase, and T_2 peaked first at one day post MCAO whereas hyperperfusion peaked at two days post MCAO. Pixel-by-pixel tracking of tissue fates showed that late hyperperfusion was associated with tissue infarction whereas tissue that was not infarcted did not show hyperperfusion (Shen et al., 2011; Tanaka et al., 2007). In short, H_2 and H2M appeared to prevent hyperperfusion which could possibly reduce reperfusion injury in the mismatch region at 1 day after MCAO.

At day 7 after MCAO, although the CBF of both the core and mismatch decreased compared to day 1 in the control group, slight hyperperfusion persisted. This is consistent with our previous studies using MR imaging on the rat MCAO model with 30–90 min occlusions, which found hyperperfusion peaked around days 1 to 2 and disappeared by day 7 (Shen et al., 2011). However, another study using 2 hr occlusion and PET imaging showed a peak of whole brain hyperperfusion of over two times control CBF at day 7 (Martin et al., 2012). One reason for this difference could be the duration of MCAO, which was 2-hours in the PET study versus 1 h in this study, and hence more severe brain damage in the former study. In our study, CBF in the mismatch was significantly different between H_2 and H2M group, and overall CBF largely normalized and was similar to CBF in the contralesional hemisphere across all 3 groups. Our finding suggests that H_2 and H2M have direct or indirect neuroprotective effects on cerebral vasculature. Hydrogen has also been shown to induce angiogenesis (Ergul et al., 2012; Zhang et al., 2019) which could be helpful to CBF recovery after stroke. However, to our knowledge, there have been no previous reports of direct or indirect improvement in CBF associated with H_2 treatment in stroke.

3.3. H_2 and H2M treatment effects on white matter integrity

The DTI (by FA, MD, AD and RD measures) provides microstructural tissue information in both gray and white matter. DTI has been used to investigate white matter and microstructural brain injury associated with ischemic stroke. In the contralesional hemisphere, all DTI parameters were normal and time invariant, except for edema which affected white matter at 1 day after MCAO. The edema effect was evident by lower FA and elevated MD, AD and RD across all three experimental groups, as expected. These group data were confirmed visually on DTI parametric maps. The edema effects were apparent as expected close to the midline of the corpus callosum.

In the ipsilesional hemisphere, the edema effects on white matter DTI parameters were expectedly greatest 1 day after MCAO across all groups. Nonetheless, most DTI parameters showed treatment effects. Specifically, at 1-day post MCAO, FA of the H2M group normalized whereas those of H_2 and control were abnormal. At 7 days post MCAO, FA of both H2M and H_2 group were normal, whereas that of control was abnormal. Similar observations were observed for MD, AD and RD. At 7 days there were less edema, the elevated RD, reduced FA, and elevated MD in controls compared to H2M might be a result of loss of white matter fiber structure. In short, H_2 treatment reduced white-matter damage and H2M treatment markedly reduced white-matter damage at both 1- and 7-day post MCAO. Our results are consistent with Hayashida et al., who found that hydrogen decreased axonal damage and neuronal degeneration, and increased neuron cell counts (Hayashida et al., 2014). There are no prior reports of direct or indirect effects on white-matter integrity in vivo associated with H_2 treatment or H2M in stroke.

The DTI (by FA, MD, AD and RD measures) provides microstructural tissue information in both gray and white matter. In our studies we observed temporally evolving edema and microstructural changes. DTI has also been used to investigate long-term microstructural changes associated with potential recovery and adaptation post stroke. These findings are in general agreement in the literature that DTI provides added value (microstructural tissue information) in addition to T2 MRI.

3.4. Limitations and future perspectives

The limitations of this study are: *i)* This pilot study employed only a single MCAO duration of 60 min and single doses of H_2 and H2M administered immediately after reperfusion and 1 and 2 days after stroke onset. Future studies will need to investigate different occlusion durations, different dosages, possible delayed treatment effects, and possible rebound edema after ending treatment after day 2. *ii)* MRI and limited behavioral measurements were made only out to 7 days, so further studies of additional behavioral measures and of and chronic effects of H2M treatment are needed. *iii)* CBF was normalized to the contralesional hemisphere in each animal to reduce inter-subject variability. However, CBF changes also occur in the contralesional hemisphere after ischemic stroke (Harston et al., 2017; Thamm et al., 2019), so our normalized CBF values cannot be interpreted relative to entirely normal CBF. *iv)* The molecular mechanisms of H_2 and minocycline alone have been previously examined, but the mechanisms of combined H2M neuroprotection have not been studied. Future studies will need to confirm if minocycline still provides anti-inflammation and anti-apoptotic effects when combined with H_2. *v)* Histological infarct volume was not assessed. However, our laboratory and others have consistently shown that T2-weighted MRI at 2 or 7 days accurately and consistently depicts histological infarct volume by hematoxylin and eosin (H&E) or triphenyl tetrazolium chloride (TTC) (Jiang et al., 2015; Shen et al., 2013). The advantage of T2 MRI for delineating lesion volume is that it can be done in vivo and longitudinally.

4. Conclusion

This is the first study of hydrogen-minocycline combination therapy in ischemic stroke. Multiparametric MRI was used to longitudinally evaluate lesion volume, tissue perfusion and white-matter integrity associated with hydrogen treatment alone and hydrogen-minocycline combination therapy of ischemic stroke. Hydrogen therapy reduced lesion volume, hyperperfusion in the ischemic penumbra, white-matter damage, and behavior deficits up to 7 days post stroke compared to vehicle-treated controls. Hydrogen and minocycline combination therapy outperformed hydrogen therapy alone. Hydrogen and minocycline individually have excellent safety profiles in humans. Hydrogen-minocycline combination therapy could potentially be administered by emergency responders in the field or during ambulance transit, enabling broad application. This warrants further investigation. These imaging approaches can also be readily translated onto clinical MRI scanners.

5. Experimental procedure

5.1. Experiment design

All experimental procedures were approved by the Institutional Animal Care and Use Committee at Stony Brook Medicine and conducted in accordance with the ARRIVE guidelines (Kilkenny et al., 2010). Male Sprague-Dawley rats (250–350 g, n = 40, Charles River Laboratories, Wilmington, MA) were randomized into three groups in a double blinded experimental design. Three animals were excluded due to surgical complication (2 from control and 1 from H2M group, all died within 3 h post-surgery) and one animal was excluded due to the absence of stroke (no diffusion abnormality at 30 mins post MCAO). The three groups and the corresponding final sample sizes for all time points were: i) control (oral water by gavage and intraperitoneal saline, n = 12), ii) H_2 (oral hydrogen water by gavage and intraperitoneal saline, n = 12), and iii) H2M (oral hydrogen water by gavage and intraperitoneal minocycline, n = 12). The final sample sizes were N = 12 for each group for reach time point. The H2 water/water alone and minocycline/saline solutions were prepared by a technician who had access to the randomization list, but who was not involved in performing experiments or analyzing data. The list was not unlocked until all the experimental procedures and data analysis were completed. The experimental design is shown in Fig. 1. The primary outcome measures were infarct volume and neurologic functional scores. The secondary outcomes were cerebral blood flow (hypo- and hyperperfusion) and white matter injury.

5.2. H_2 water preparation

Hydrogen-enriched water was prepared by using hydrogen-producing tablets (Rejuvenation H_2 tablets), kindly donated by Drink HRW (Port Hueneme, CA). Each tablet contains 80 mg of magnesium, which reacts with water to produce hydrogen gas (LeBaron et al., 2019). A single tablet was dissolved in 250 ml water in a stainless steel can with a tightly-fitted stainless steel lid, producing hydrogen-enriched water containing a near saturated concentration of dissolved hydrogen (up to 1.6 ppm at room temperature and pressure), as verified using a dissolved hydrogen-measuring electrode (Sata Shouji ENH-1000, Kawasaki City, Japan; accuracy ± 5 ppb) or a hydrogen test kit (H_2Blue, H_2 Sciences Inc., Henderson, NV). After opening the sealed can, hydrogen-enriched water was administered as quickly as possible to minimize dissipation of dissolved hydrogen, using gastric gavage at a dose of 10 ml/kg.

5.3. H_2 water and minocycline dose selection

A typical neuroprotective dose of H_2 water or saline in the recent animal research literatures is 10 ml/kg qd (Li et al., 2018; Meng et al., 2015; Zhou et al., 2013). A 10 ml/kg dose was found to provide better protection than a dose of 5 ml/kg against spinal cord injury in rabbits (Zhou et al., 2013). In our study with an average adult male rat weight of around 300 g, the 10 ml/kg corresponded to about 3 ml of H_2 water by oral gavage. This dose fits within the therapeutic ranges previously reported, including 3 ml of 50% saturated water by gavage in rats used by Fu et al (Fu et al., 2009) that gave similar blood H_2 levels as the 2% H_2 gas inhalation used by Ohsawa et al (Ohsawa et al., 2007), who found both 2% and 4% H_2 inhalation to be protective in a rat permanent MCAO stroke model. Therefore, a 10 ml/kg dose of a near saturated concentration of dissolved hydrogen (up to 1.6 ppm at room temperature and pressure) was selected in present study.

The effective dose for minocycline for neuroprotection in stroke was reported to be between 10 and 100 mg/kg for intraperitoneal administration (Naderi et al., 2020). For combination therapy in this study to enhance hydrogen's anti-inflammation and antioxidant effects, a dose in the lower range for minocycline was used, 20 mg/kg.

5.4. Animal preparation

The animals were intubated and mechanically ventilated under isoflurane (2% in room air). MCAO was achieved by inserting an intraluminal silicon rubber-coated filament (Doccol Corporation, Sharon, MA) through the right external carotid artery in a retrograde fashion. The animals were then secured in the supine position using a custom-made MRI-compatible stereotaxic headset. After the initial MRI measurements at 20–40 mins after onset of stroke, rats were taken out from the MRI scanner and reperfused 60 mins after MCAO. Subsequently, hydrogen water was given by gastric gavage at a dose of 10mk/kg, and minocycline (Sigma-Aldrich, St. Louis, MO, USA) was administered i.p.

at a dose of 20 mg/kg immediately after reperfusion. Treatments were repeated again 1 day and 2 days after MCAO.

End-tidal CO_2 was monitored via a SurgiVet capnometer (Smith Medical, Waukesha, WI, USA). Rectal temperature (36.0–37.0 °C), heart rate (300–350 bpm), respiration rate (55–65/min) and arterial oxygenation saturation (90–99%) were recorded using an MRI-compatible monitoring system (Small Animal Instrument, Stony Brook, NY, USA) and maintained within normal physiological range during MRI scanning. All rats were housed with companions before the MCAO but alone afterwards, in a 12-12 h light/dark circle room with constant temperature (22 ± 2℃) and humidity (55 ± 10%). All animals had free access to food and water.

5.5. MRI experiments

MRI was performed on a Bruker Biospec 7.0 T/20 cm scanner with a 66G/cm BGA12SHP gradient (Billerica, MA) using a custom-made surface coil (2.3 cm inner diameter) for brain imaging and a neck coil for perfusion labeling. Diffusion and blood flow MRI were acquired at 30 mins, 90 mins, 1 day and 7 days after MCAO. T_2 maps were acquired on 1 and 7 days after MCAO.

Cerebral blood flow (CBF) was measured using the continuous arterial spin-labeling (cASL) technique with gradient echo-planar imaging (Shen et al., 2013). Labeling duration was 1.7 s and post-labeling delay was 250 ms. Acquisition parameters were matrix = 96x96 with partial Fourier (5/8) acquisition and reconstructed to 128x128, field of view (FOV) = 25.6x25.6 mm, five 1.5 mm slices, repetition time (TR) = 2200 ms, 90° flip angle, and echo time (TE) = 9.5 ms.

Diffusion Tensor Imaging (DTI) was measured using spin-echo diffusion-weighted echo-planar imaging with gradients separately applied along three orthogonal directions (Shen et al., 2013). Two b values of 4 and 1,200 s/mm^2 were used with Δ = 8.4 ms, δ = 2.5 ms, and 30 directions. Other MRI parameters were: single shot, matrix = 96x96 (reconstructed to 128 × 128), FOV = 25.6 × 25.6 mm, five 1.5 mm thick slices, 90° flip angle, TR = 3000 ms, TE = 25 ms.

T_2-weighted images were acquired using fast spin-echo pulse sequence (Shen et al., 2013) with four effective echo times (25 ms and 75 ms, 40 ms and 120 ms, two separate acquisitions), TR = 3000 ms (90° flip angle), matrix = 128 × 128, FOV = 25.6 × 25.6 mm, RARE factor of 6, and 8 signal averages.

5.6. MRI analysis

Data analysis used codes written in Matlab (MathWorks, Natick, MA, USA) and Mango (University of Texas at San Antonio, San Antonio, TX, USA) software. Images from each rat at different time points were co-registered. CBF and T_2 maps were calculated. From DTI, Apparent diffusion coefficient (ADC), Fractional anisotropy (FA), Axial Diffusivity (AD), Radial Diffusivity (RD), and Mean Diffusivity (MD) were calculated. The initial lesion volume was defined by the ADC lesion 30 mins post stroke using a threshold of the mean ADC of the normal hemisphere minus 3x the standard deviation (Rodriguez et al., 2016). A threshold of 0.30 ml/g/min was used to define the CBF deficit tissue volume (Shen et al., 2013). The perfusion-diffusion mismatch was taken to be tissue with ADC above threshold but with CBF below threshold. For CBF analysis, both quantitative and normalized CBF with respect to the contralesional (normal) ROIs were used.

Athough there are changes in the contralesional hemisphere at the miscroscopic and molecular level. At the macroscopic level of CBF, there was relatively little or no changes in the majority of the contralesional hemisphere (Harston et al., 2017; Thamm et al., 2019). Thus, for comparison purpose across groups within a study, normalization to contralesional hemisphere CBF values avoids the large inter-subject variability if we were to compare to a sham group as we have done previously (Jiang et al., 2015).

Lesion volumes defined by abnormal ADC were tabulated longitudinally. Infarct volumes at 1 and 7 days after MCAO were defined by T_2 using the threshold of mean T_2 of the normal hemisphere plus two times the standard deviation. Edema-corrected infarct volume was calculated (Shen et al., 2013).

CBF of the ischemic core and perfusion-diffusion mismatch were tracked longitudinally using ROIs identified as core and mismatched at 30 mins.

For white matter assessment, ROIs of the corpus callosum (CC) on ipsilesional and contralesional hemisphere to stroke were drawn based on FA maps at each time point. FA, MD, AD and RD values were analyzed for both sides of CC for individual animals, followed by group averaging.

5.7. Neurological deficits

The Garcia neurological test was used to determine behavioral neurological deficits (Jiang et al., 2015). Briefly, the Garcia test consists of spontaneous activity, tail suspension movement of all limbs, forelimb outstretching, climbing, touching of trunk, and vibrissae touching. Individual tests were scored from 1 to 3 (3 is best) and summed to constitute a 6–18 point total. Higher scores represent milder neurological deficits. Garcia scores were assessed blinded to treatment group 1 and 7 days after MCAO, prior to the MRI scans.

5.8. Statistical analysis

Data in text and plots are shown as mean ± STD. For lesion volume, a two-way repeated-measures ANOVA analysis was used for comparison across different groups at each time point, and followed by post hoc analysis using t-tests (with Bonferroni-Holm correction) comparing groups at 1 and 7 days after stroke. The same analysis was used for other MRI parameters. Neurological scores were analyzed similarly with data only from 1 and 7 days after stroke. $p < 0.05$ was considered significant.

CRediT authorship contribution statement

Zhao Jiang: Conceptualization, Investigation, Methodology, Data curation, Formal analysis, Writing - original draft, Writing - review & editing. **Tharun T. Alamuri:** Formal analysis, Writing - original draft, Writing - review & editing. **Eric R. Muir:** Formal analysis, Data curation, Writing - review & editing. **Dennis W. Choi:** Conceptualization, Resources, Writing - review & editing. **Tim Q. Duong:** Conceptualization, Resources, Data curation, Writing - review & editing.

Declaration of Competing Interest

The authors declare that they have no known competing financial interests or personal relationships that could have appeared to influence the work reported in this paper.

References

Ackerman, R.H., Correia, J.A., Alpert, N.M., Baron, J.C., Gouliamos, A., Grotta, J.C., et al., 1981. Positron imaging in ischemic stroke disease using compounds labeled with oxygen 15. Initial results of clinicophysiologic correlations. Arch. Neurol. 38 (9), 537–543.

Albers, G.W., 1999. Expanding the window for thrombolytic therapy in acute stroke: The potential role of acute MRI for patient selection. Stroke 30, 2230–2237.

Astrup, J., Sorensen, P.M., Sorensen, H.R., 1981a. Oxygen and glucose consumption related to Na+/K+ transport in canine brain. Stroke 12, 726–730.

Astrup, J., Symon, L., Siesjo, B.K., 1981b. Thresholds in cerebral ischemia: the ischemic penumbra. Stroke 12, 723–725.

Baron, J.C., Bousser, M.G., Comar, D., Soussaline, F., Castaigne, P., 1981. Noninvasive tomographic study of cerebral blood flow and oxygen metabolism in vivo. Potentials, limitations, and clinical applications in cerebral ischemic disorders. Eur. Neurol. 20 (3), 273–284.

Baron, J.C., Delattre, J.Y., Bories, J., Chiras, J., Cabanis, E.A., Blas, C., et al., 1983.

Comparison study of CT and positron emission tomographic data in recent cerebral infarction. AJNR Am. J. Neuroradiol. 4 (3), 536–540.
Chan, P.H., 2001. Reactive oxygen radicals in signaling and damage in the ischemic brain. J. Cereb. Blood Flow Metab. 21 (1), 2–14. https://doi.org/10.1097/00004647-200101000-00002.
Chaturvedi, M., Kaczmarek, L., 2014. Mmp-9 inhibition: a therapeutic strategy in ischemic stroke. Mol. Neurobiol. 49 (1), 563–573. https://doi.org/10.1007/s12035-013-8538-z.
Coyle, J.T., Puttfarcken, P., 1993. Oxidative stress, glutamate, and neurodegenerative disorders. Science 262 (5134), 689–695. https://doi.org/10.1126/science.7901908.
Cui, Y., Zhang, H., Ji, M., Jia, M., Chen, H., Yang, J., Duan, M., 2014. Hydrogen-rich saline attenuates neuronal ischemia–reperfusion injury by protecting mitochondrial function in rats. J. Surg. Res. 192 (2), 564–572. https://doi.org/10.1016/j.jss.2014.05.060.
Davis, S.M., Donnan, G.A., 2009. 4.5 hours: the new time window for tissue plasminogen activator in stroke. Stroke 40 (6), 2266–2267 STROKEAHA.108.544171 [pii] 1161/STROKEAHA.108.544171 [doi].
Dawson, T.M., Dawson, V.L., 2018. Nitric oxide signaling in neurodegeneration and cell death. Adv. Pharmacol. 82, 57–83. https://doi.org/10.1016/bs.apha.2017.09.003.
Ergul, A., Alhusban, A., Fagan, S.C., 2012. Angiogenesis: a harmonized target for recovery after stroke. Stroke 43 (8), 2270–2274. https://doi.org/10.1161/STROKEAHA.111.642710.
Fagan, S.C., Cronic, L.E., Hess, D.C., 2011. Minocycline development for acute ischemic stroke. Transl. Stroke Res. 2 (2), 202–208. https://doi.org/10.1007/s12975-011-0072-6.
Feng, S., Yang, Q., Liu, M., Li, W., Yuan, W., Zhang, S., et al., 2011. Edaravone for acute ischaemic stroke. Cochrane Database Syst. Rev. 12, CD007230. https://doi.org/10.1002/14651858.CD007230.pub2.
Fu, Y., Ito, M., Fujita, Y., Ito, M., Ichihara, M., Masuda, A., et al., 2009. Molecular hydrogen is protective against 6-hydroxydopamine-induced nigrostriatal degeneration in a rat model of Parkinson's disease. Neurosci. Lett. 453 (2), 81–85. https://doi.org/10.1016/j.neulet.2009.02.016.
Ginsberg, M.D., 2009. Current status of neuroprotection for cerebral ischemia: synoptic overview. Stroke 40 (3 Suppl), S111–114. https://doi.org/10.1161/STROKEAHA.108.528877.
Harston, G.W., Okell, T.W., Sheerin, F., Schulz, U., Mathieson, P., Reckless, I., et al., 2017. Quantification of serial cerebral blood flow in acute stroke using arterial spin labeling. Stroke 48 (1), 123–130. https://doi.org/10.1161/STROKEAHA.116.014707.
Hayashida, K., Sano, M., Kamimura, N., Yokota, T., Suzuki, M., Ohta, S., et al., 2014. Hydrogen inhalation during normoxic resuscitation improves neurological outcome in a rat model of cardiac arrest independently of targeted temperature management. Circulation 130 (24), 2173–2180. https://doi.org/10.1161/CIRCULATIONAHA.114.011848.
Hewlett, K.A., Corbett, D., 2006. Delayed minocycline treatment reduces long-term functional deficits and histological injury in a rodent model of focal ischemia. Neuroscience 141 (1), 27–33. https://doi.org/10.1016/j.neuroscience.2006.03.071.
Hossmann, K.-A., 1994. Viability Thresholds and the Penumbra of Focal Ischemia. Ann. Neurol. 36, 557–565.
Huang, L., Lu, J., Cerqueira, B., Liu, Y., Jiang, Z., Duong, T.Q., 2018. Chronic oral methylene blue treatment in a rat model of focal cerebral ischemia/reperfusion. Brain Res. 1678, 322–329.
Hugyecz, M., Mracsko, E., Hertelendy, P., Farkas, E., Domoki, F., Bari, F., 2011. Hydrogen supplemented air inhalation reduces changes of prooxidant enzyme and gap junction protein levels after transient global cerebral ischemia in the rat hippocampus. Brain Res. 1404, 31–38. https://doi.org/10.1016/j.brainres.2011.05.068.
Iadecola, C., Alexander, M., 2001. Cerebral ischemia and inflammation. Curr. Opin. Neurol. 14 (1), 89–94. https://doi.org/10.1097/00019052-200102000-00014.
Jiang, Z., Watts, L.T., Huang, S., Shen, Q., Rodriguez, P., Chen, C., et al., 2015. The effects of methylene blue on autophagy and apoptosis in MRI-defined normal tissue, ischemic penumbra and ischemic core. PLoS ONE 10 (6), e0131929.
Jin, Z., Liang, J., Wang, J., Kolattukudy, P.E., 2015. MCP-induced protein 1 mediates the minocycline-induced neuroprotection against cerebral ischemia/reperfusion injury in vitro and in vivo. J Neuroinflammation 12, 39. https://doi.org/10.1186/s12974-015-0264-1.
Kidwell, C.S., Alger, J.R., Saver, J.L., 2003. Beyond mismatch: evolving paradigms in imaging the ischemic penumbra with multimodal magnetic resonance imaging. Stroke 34 (11), 2729–2735.
Kidwell, C.S., Saver, J.L., Mattiello, J., Starkman, S., Vinuela, F., Duckwiler, G., et al., 2000. Thrombolytic reversal of acute human cerebral ischemia injury shown by diffusion/perfusion magnetic resonance imaging. Ann. Neurol. 47, 462–469.
Kidwell, C.S., Saver, J.L., Mattiello, J., Starkman, S., Vinuela, F., Duckwiller, G., et al., 2001. Diffusion-perfusion MRI characterization of post-recanalization hyperperfusion in humans. Neurology 57, 2015–2021.
Kilkenny, C., Browne, W.J., Cuthill, I.C., Emerson, M., Altman, D.G., 2010. Improving bioscience research reporting: the ARRIVE guidelines for reporting animal research. PLoS Biol. 8 (6), e1000412. https://doi.org/10.1371/journal.pbio.1000412.
Koh, J.Y., Suh, S.W., Gwag, B.J., He, Y.Y., Hsu, C.Y., Choi, D.W., 1996. The role of zinc in selective neuronal death after transient global cerebral ischemia. Science 272 (5264), 1013–1016. https://doi.org/10.1126/science.272.5264.1013.
Kuroda, S., Siesjo, B.K., 1997. Reperfusion damage following focal ischemia: pathophysiology and therapeutic windows. Clin. Neurosci. 4 (4), 199–212.
LeBaron, T.W., Larson, A.J., Ohta, S., Mikami, T., Barlow, J., Bulloch, J., DeBeliso, M., 2019. Acute supplementation with molecular hydrogen benefits submaximal exercise indices. randomized, double-blinded, placebo-controlled crossover pilot study. J Lifestyle Med 9 (1), 36–43. https://doi.org/10.15280/jlm.2019.9.1.36.
Li, F., Gong, Q., Wang, L., Shi, J., 2012. Osthole attenuates focal inflammatory reaction following permanent middle cerebral artery occlusion in rats. Biol. Pharm. Bull. 35 (10), 1686–1690. https://doi.org/10.1248/bpb.b12-00133.
Li, H., Bai, G., Ge, Y., Zhang, Q., Kong, X., Meng, W., Wang, H., 2018. Hydrogen-rich saline protects against small-scale liver ischemia-reperfusion injury by inhibiting endoplasmic reticulum stress. Life Sci. 194, 7–14. https://doi.org/10.1016/j.lfs.2017.12.022.
Li, H., Luo, Y., Yang, P., Liu, J., 2019. Hydrogen as a complementary therapy against ischemic stroke: a review of the evidence. J. Neurol. Sci. 396, 240–246. https://doi.org/10.1016/j.jns.2018.11.004.
Liu, Y., Liu, W., Sun, X., Li, R., Sun, Q., Cai, J., et al., 2011. Hydrogen saline offers neuroprotection by reducing oxidative stress in a focal cerebral ischemia-reperfusion rat model. Med. Gas Res. 1 (1), 15. https://doi.org/10.1186/2045-9912-1-15.
Lo, E.H., Moskowitz, M.A., Jacobs, T.P., 2005. Exciting, radical suicidal: how brain cell die after stroke. Stroke 36, 189–192.
Lu, Y., Xiao, G., Luo, W., 2016. Minocycline suppresses NLRP3 inflammasome activation in experimental ischemic stroke. NeuroImmunoModulation 23 (4), 230–238. https://doi.org/10.1159/000452172.
Malhotra, K., Chang, J.J., Khunger, A., Blacker, D., Switzer, J.A., Goyal, N., et al., 2018. Minocycline for acute stroke treatment: a systematic review and meta-analysis of randomized clinical trials. J. Neurol. 265 (8), 1871–1879. https://doi.org/10.1007/s00415-018-8935-3.
Marchal, G., Furlan, M., Beaudouin, V., Rioux, P., Hauttement, J.L., Serrati, C., et al., 1996. Early spontaneous hyperperfusion after stroke. A marker of favourable tissue outcome? Brain 119 (Pt 2), 409–419.
Martin, A., Mace, E., Boisgard, R., Montaldo, G., Theze, B., Tanter, M., Tavitian, B., 2012. Imaging of perfusion, angiogenesis, and tissue elasticity after stroke. J. Cereb. Blood Flow Metab. 32 (8), 1496–1507. https://doi.org/10.1038/jcbfm.2012.49.
Meng, X., Chen, H., Wang, G., Yu, Y., Xie, K., 2015. Hydrogen-rich saline attenuates chemotherapy-induced ovarian injury via regulation of oxidative stress. Exp. Ther. Med. 10 (6), 2277–2282. https://doi.org/10.3892/etm.2015.2787.
Minematsu, K., Fisher, M., Li, F., Sotak, C.H., 1993. Diffusion and perfusion magnetic resonance imaging studies to evaluate a noncompetitive N-Methyl-d-aspartate antagonist and reperfusion in experimental stroke in rats. Stroke 24, 2074–2081.
Monyer, H., Hartley, D.M., Choi, D.W., 1990. 21-Aminosteroids attenuate excitotoxic neuronal injury in cortical cell cultures. Neuron 5 (2), 121–126. https://doi.org/10.1016/0896-6273(90)90302-v.
Moseley, M., Chew, M.E., White, W.M., Kucharczyk, D.L., Litt, J., Derugin, L., et al., 1992. Hypercarbia-induced changes in cerebral blood volume in the cat: A 1H MRI and intravascular contrast agent study. Magn. Reson. Med. 23, 21–30.
Moseley, M.E., Cohen, Y., Mintorovitch, J., Chileuitt, L., Shimizu, H., Kucharczyk, J., et al., 1990. Early detection of regional cerebral ischemia in cats: comparison of diffusion- and T2-weighted MRI and spectroscopy. Magn. Reson. Med. 14 (2), 330–346.
Naderi, Y., Panahi, Y., Barreto, G.E., Sahebkar, A., 2020. Neuroprotective effects of minocycline on focal cerebral ischemia injury: a systematic review. Neural Regen. Res. 15 (5), 773–782. https://doi.org/10.4103/1673-5374.268898.
Naderi, Y., Sabetkasaei, M., Parvardeh, S., & Moini Zanjani, T., 2017. Neuroprotective effects of pretreatment with minocycline on memory impairment following cerebral ischemia in rats. Behav Pharmacol, 28(2 and 3-Spec Issue), 214-222. doi:10.1097/FBP.0000000000000297.
Nemeth, J., Toth-Szuki, V., Varga, V., Kovacs, V., Remzso, G., Domoki, F., 2016. Molecular hydrogen affords neuroprotection in a translational piglet model of hypoxic-ischemic encephalopathy. J. Physiol. Pharmacol. 67 (5), 677–689.
Ohsawa, I., Ishikawa, M., Takahashi, K., Watanabe, M., Nishimaki, K., Yamagata, K., et al., 2007. Hydrogen acts as a therapeutic antioxidant by selectively reducing cytotoxic oxygen radicals. Nat. Med. 13 (6), 688–694. https://doi.org/10.1038/nm1577.
Ohta, S., 2014. Molecular hydrogen as a preventive and therapeutic medical gas: initiation, development and potential of hydrogen medicine. Pharmacol. Ther. 144 (1), 1–11. https://doi.org/10.1016/j.pharmthera.2014.04.006.
Ono, H., Nishijima, Y., Ohta, S., Sakamoto, M., Kinone, K., Horikosi, T., et al., 2017. Hydrogen gas inhalation treatment in acute cerebral infarction: a randomized controlled clinical study on safety and neuroprotection. J. Stroke Cerebrovasc Dis. 26 (11), 2587–2594. https://doi.org/10.1016/j.jstrokecerebrovasdis.2017.06.012.
Pan, J., Konstas, A.A., Bateman, B., Ortolano, G.A., Pile-Spellman, J., 2007. Reperfusion injury following cerebral ischemia: pathophysiology, MR imaging, and potential therapies. Neuroradiology 49 (2), 93–102.
Rodriguez, P., Zhao, J., Milman, B., Tiwari, Y.V., Duong, T.Q., 2016. Methylene blue and normobaric hyperoxia combination therapy in experimental ischemic stroke. Brain and behavior 6 (7), e00478.
Schaller, B., Graf, R., 2004. Cerebral ischemia and reperfusion: the pathophysiologic concept as a basis for clinical therapy. J. Cereb. Blood Flow Metab. 24 (4), 351–371.
Sheline, C.T., Wang, H., Cai, A.L., Dawson, V.L., Choi, D.W., 2003. Involvement of poly ADP ribosyl polymerase-1 in acute but not chronic zinc toxicity. Eur. J. Neurosci. 18 (6), 1402–1409. https://doi.org/10.1046/j.1460-9568.2003.02865.x.
Shen, Q., Du, F., Huang, S., Duong, T.Q., 2011. Spatiotemporal characteristics of post-ischemic hyperperfusion with respect to changes in T1, T2, diffusion, angiography, and blood-brain barrier permeability. J. Cereb. Blood Flow Metab. 31 (10), 2076–2085. https://doi.org/10.1038/jcbfm.2011.64.
Shen, Q., Du, F., Huang, S., Rodriguez, P., Watts, L.T., Duong, T.Q., 2013. Neuroprotective efficacy of methylene blue in ischemic stroke: an MRI study. PLoS ONE 8 (11), e79833. https://doi.org/10.1371/journal.pone.0079833.
Sheng, Z., Liu, Y., Li, H., Zheng, W., Xia, B., Zhang, X., et al., 2018. Efficacy of minocycline in acute ischemic stroke: a systematic review and meta-analysis of rodent and clinical studies. Front. Neurol. 9, 1103. https://doi.org/10.3389/fneur.2018.01103.
Sorensen, A., Buonanno, F., Gonzalez, R., 1996. Hyperacute stroke; evaluation with

combined multisection diffusion-weighted and hemoddynamically weighted echo-planar imaging. Radiology 199, 391–401.
Sorensen, A.G., Copen, W., Ostergaard, L., Buoonanno, F., Gonzalez, R.G., Rordorf, G., et al., 1999. Hyperacute stroke: Simultaneous measurement of relative cerebral blood volume, relative cerebral blood flow, and mean tissue transit time. Radiology 210, 519–527.
Sundt Jr., T.M., Grant, W.C., Garcia, J.H., 1969. Restoration of middle cerebral artery flow in experimental infarction. J. Neurosurg. 31 (3), 311–321. https://doi.org/10.3171/jns.1969.31.3.0311.
Tanaka, M., Ishihara, Y., Mizuno, S., Ishida, A., Vogel, C.F., Tsuji, M., et al., 2018. Progression of vasogenic edema induced by activated microglia under permanent middle cerebral artery occlusion. Biochem. Biophys. Res. Commun. 496 (2), 582–587. https://doi.org/10.1016/j.bbrc.2018.01.094.
Tanaka, Y., Ishii, H., Hiraoka, M., Miyasaka, N., Kuroiwa, T., Hajjar, K.A., et al., 2007. Efficacy of recombinant annexin 2 for fibrinolytic therapy in a rat embolic stroke model: A magnetic resonance imaging study. Brain Res. 1165, 135–143.
Tasdemiroglu, E., Macfarlane, R., Wei, E.P., Kontos, H.A., Moskowitz, M.A., 1992. Pial vessel caliber and cerebral blood flow become dissociated during ischemia-reperfusion in cats. Am. J. Physiol. 263 (2 Pt 2), H533–536.
Thamm, T., Guo, J., Rosenberg, J., Liang, T., Marks, M.P., Christensen, S., et al., 2019. Contralateral hemispheric cerebral blood flow measured with arterial spin labeling can predict outcome in acute stroke. Stroke 50 (12), 3408–3415. https://doi.org/10.1161/STROKEAHA.119.026499.
Tran Dinh, Y.R., Ille, O., Guichard, J.P., Haguenau, M., Seylaz, J., 1997. Cerebral post-ischemic hyperperfusion assessed by Xenon-133 SPECT. J. Nucl. Med. 38 (4), 602–607.
Warach, S., 2003. Measurement of the ischemic penumbra with MRI: it's about time. Stroke 34, 2533–2534.
Xu, L., Fagan, S.C., Waller, J.L., Edwards, D., Borlongan, C.V., Zheng, J., et al., 2004. Low dose intravenous minocycline is neuroprotective after middle cerebral artery occlusion-reperfusion in rats. BMC Neurol. 4, 7. https://doi.org/10.1186/1471-2377-4-7.
Yrjanheikki, J., Tikka, T., Keinanen, R., Goldsteins, G., Chan, P.H., Koistinaho, J., 1999. A tetracycline derivative, minocycline, reduces inflammation and protects against focal cerebral ischemia with a wide therapeutic window. Proc. Natl. Acad. Sci. USA 96 (23), 13496–13500. https://doi.org/10.1073/pnas.96.23.13496.
Zhang, G., Li, Z., Meng, C., Kang, J., Zhang, M., Ma, L., Zhou, H., 2018. The anti-inflammatory effect of hydrogen on lung transplantation model of pulmonary microvascular endothelial cells during cold storage period. Transplantation 102 (8), 1253–1261. https://doi.org/10.1097/TP.0000000000002276.
Zhang, Z.Y., Fang, Y.J., Luo, Y.J., Lenahan, C., Zhang, J.M., Chen, S., 2019. The role of medical gas in stroke: an updated review. Med. Gas Res. 9 (4), 221–228. https://doi.org/10.4103/2045-9912.273960.
Zhou, L., Wang, X., Xue, W., Xie, K., Huang, Y., Chen, H., et al., 2013. Beneficial effects of hydrogen-rich saline against spinal cord ischemia-reperfusion injury in rabbits. Brain Res. 1517, 150–160. https://doi.org/10.1016/j.brainres.2013.04.007.